

## APSIDAL MOTION AND A LIGHT CURVE SOLUTION FOR THIRTEEN LMC ECCENTRIC ECLIPSING BINARIES

P. ZASCHE<sup>1</sup>, M. WOLF<sup>1</sup>, J. VRAŠTIL<sup>1</sup>, L. PILARČÍK<sup>1</sup>

<sup>1</sup> Astronomical Institute, Charles University in Prague, Faculty of Mathematics and Physics,  
CZ-180 00 Praha 8, V Holešovičkách 2, Czech Republic

*Draft version December 15, 2015*

### ABSTRACT

New CCD observations for thirteen eccentric eclipsing binaries from the Large Magellanic Cloud were carried out using the Danish 1.54-meter telescope located at the La Silla Observatory in Chile. These systems were observed for their times of minima and 56 new minima were obtained. These are needed for accurate determination of the apsidal motion. Besides that, in total 436 times of minima were derived from the photometric databases OGLE and MACHO. The  $O - C$  diagrams of minima timings for these B-type binaries were analysed and the parameters of the apsidal motion were computed. The light curves of these systems were fitted using the program PHOEBE, giving the light curve parameters. We derived for the first time the relatively short periods of the apsidal motion ranging from 21 to 107 years. The system OGLE-LMC-ECL-07902 was also analysed using the spectra and radial velocities, resulting in masses 6.8, and 4.4  $M_{\odot}$  for the eclipsing components. For one system (OGLE-LMC-ECL-20112), the third-body hypothesis was also used for describing the residuals after subtraction of the apsidal motion, resulting in period of about 22 years. For several systems an additional third light was also detected, which makes these systems suspicious of triplicity.

*Subject headings:* stars: binaries: eclipsing – stars: early-type – stars: fundamental parameters – Magellanic Clouds

### 1. INTRODUCTION

In some aspects the focus of astronomers to eclipsing binaries moved from the galactic to extragalactic targets. This is mainly due to the large and long-lasting photometric monitoring projects. Such surveys like MACHO or OGLE have discovered many thousands of new eclipsing binaries in both Large and Small Magellanic Clouds, hence, we know only about twice more eclipsing binaries in our own Milky Way than in other galaxies (see Pawlak et al. 2013, or Graczyk et al. 2011).

The role of eclipsing binaries to our current astrophysical knowledge is undisputable. For example the eccentric eclipsing binaries (hereafter EEBs) with an apsidal motion can provide us with an important observational test of theoretical models of stellar structure and evolution. A long-term collection of the times of EEBs minima observed for several years during its apsidal motion cycle and their analysis can provide us with both the orbital eccentricity and the period of rotation of the apsidal line with high accuracy (Giménez 1994). Many different sets of stellar evolution models have been published in recent years, such as Maeder (1999), Claret (2005), the MESA code (Paxton et al. 2011), the  $Y^2$  models (Demarque et al. 2004), or others. However, to distinguish between them and to test, which one is more suitable, it is still rather difficult (see e.g. Martins & Palacios 2013). The internal structure constants, as derived from the apsidal motion analysis, could serve as one independent criterion which can be used. However, to discriminate between the models one would need an accuracy of internal structure constants of about 1%, which can be achieved only with very precise photometric and spectroscopic data.

However, the chemical composition of the Magellanic Clouds differs a bit from that of our solar neighborhood (see e.g. Westerlund 1997, or Davies et al. 2015), and

the study of the massive and metal-deficient stars in the Magellanic Clouds checks our evolutionary models for these abundances. All of the eclipsing binaries analysed in the present study have properties that make them important astrophysical laboratories for studying the stellar structure and evolution of massive stars (Ribas 2004).

In the following sections we analyse the photometric data obtained during the automatic survey as well as our own observations and derive the rates of apsidal motion for thirteen detached eclipsing systems with eccentric orbits located in the Large Magellanic Cloud. All these systems are early-type objects, exhibit an apsidal motion, and was only poorly studied until now. Similar studies of LMC EEBs have been presented by Michalska & Pigulski (2005), by Michalska (2007), by Zasche & Wolf (2013), and recently also by Hong et al. (2014). A set of such binaries with known apsidal motion is still rather limited outside of our Galaxy, hence a new contribution to the topic is still very important. It can also serve as a testing benchmark or a starting point for some future more detailed investigation of such systems.

### 2. OBSERVATIONS OF MINIMUM LIGHT

The analysis of mid-eclipse times measurements became a popular method nowadays, especially thanks to the superb precision and a time coverage of the Kepler targets, see e.g. Borkovits et al. (2015). Moreover, such a photometric monitoring of faint EEBs in external galaxies became almost routine nowadays with quite modest telescopes of 1 - 2m class, which are equipped with a modern CCD camera. However, a large amount of observing time is needed, which is usually unavailable at larger telescopes. This especially apply for spectroscopy and other more challenging techniques, for the photometry the situation is much more promising.

Therefore, during the last three observational seasons,

we have accumulated many photometric observations and derived 56 precise times of minimum light for selected eccentric systems. The systems for our presented analysis were chosen following an easy criterion: all of them were already observed during the previous seasons in the fields of the already known apsidal motion stars in the LMC. New CCD photometry was obtained at the La Silla Observatory in Chile, where the 1.54-m Danish telescope (hereafter DK154) with the CCD camera and  $R$  filter was used (remotely operated from the Czech Republic).

A standard procedure for the reduction was used, applying the bias frames and then the flat fields to the CCD frames. The comparison star was chosen to be close to the variable one and with similar spectral type. A custom-made aperture-photometry reduction software APHOT developed by M. Velen and P. Pravec, was routinely used for reducing the data. No correction for differential extinction was applied because of the proximity of the comparison stars to the variable and the resulting negligible differences in air mass and their similar spectral types.

The new times of primary and secondary minima and their respective errors were determined by the classical Kwee-van Woerden (1956) method or by our new approach (see Zasche et al. 2014). All new times of minima are given in the online-only appendix Table 1.

### 3. PHOTOMETRY AND LIGHT CURVE MODELLING

The main part of our present analysis lies on the huge photometric data sets as obtained during the MACHO and OGLE surveys. From these large surveys the photometric catalogues with thousands of eclipsing binaries were used for our analysis, namely: the MACHO (Faccioli et al. 2007), OGLE II (Wyrzykowski et al. 2004), and OGLE III (Graczyk et al. 2011) databases. These data were used both for analysing the minima times as well as for the analysis of the light curve. Our new observations carried out with the DK154 were used only to derive the times of minimum light for the studied systems because only small parts of the light curves near the minima were observed.

The light curve (hereafter LC) analysis for a particular system was carried out using the program PHOEBE, ver. 0.31a (Prša & Zwitter 2005), which is based on the Wilson-Devinney algorithm (Wilson & Devinney 1971) and its later modifications. However, some of the parameters have to be fixed during the fitting process. The albedo coefficients  $A_i$  remained fixed at a value 1.0, the gravity darkening coefficients  $g_i = 1.0$ . The limb darkening coefficients were interpolated from the van Hamme tables (van Hamme 1993), and the synchronicity parameters ( $F_i$ ) were also kept fixed at values of  $F_i = 1$ . The temperature of the primary component was derived from the photometric indices. The  $(B - V)_0$  and  $(V - I)_0$  indices were used for the estimation of the primary temperature (see the next paragraph), see the Table 2. Hence, the set of parameters derived during the LC fitting of all the systems is the following: secondary temperature  $T_2$ , inclination  $i$ , the Kopal's modified potentials  $\Omega_i$ , and the luminosities  $L_i$ .

The proper primary temperature was mostly found by using the photometric indices as published by the OGLE team (see Table 2), or by using the  $UBV$  magnitudes as

published by Massey (2002), or Zaritsky et al. (2004). After then, the dereddened indices (using the method by Johnson 1958) were used for estimation of a spectral type and roughly also its temperature (e.g. from Pecaut & Mamajek 2013). The similar method was also used for the  $(V - I)_0$  indices, while the  $E(V - I)$  was taken as an average of the  $E(V - I)$  values given by Ulaczyk et al. (2012). All of these binaries seem to be of B1-B9 spectral type.

The problematic issue of the mass ratio (without having any spectroscopy) was solved in the following way. Because the detached eclipsing binaries and their LC solution is only poorly sensitive to the photometric mass ratio (see e.g. Terrell & Wilson 2005), we used a different approach as described e.g. in Graczyk (2003). In this approach, we assume that the stars follow a standard mass-luminosity relation and hence the estimated mass ratio can be derived from the following equation:

$$q = 10^{(\log L_2 - \log L_1)/3.664},$$

where the luminosity values of the two components were taken from the LC solution from PHOEBE. Using this method iteratively, we obtain a new photometric mass ratio after only a few steps (usually three to five). Such a value of  $q$  is physically self-consistent with the derived values of radii, luminosities, etc.

Here we would like to point out that the solution found with the PHOEBE program is a formal one, based on the abovementioned assumptions (the inclusion of some future knowledge of these stars can significantly shift our solution). Moreover, also the errors as resulted from the code are purely mathematical ones and usually are strongly underestimated in the PHOEBE program (Prša & Zwitter 2005, or PHOEBE manual<sup>1</sup>).

### 4. APSIDAL MOTION ANALYSIS

For the analysis of period changes using the times of minima, we used the approach as presented below.

1. At first, all photometric data were analysed, resulting in a set of preliminary minima times. Hence, also some preliminary apsidal motion parameters were derived (with the assumption  $i = 90^\circ$ ).
2. At second, the eccentricity ( $e$ ), argument of periastron ( $\omega$ ), and the apsidal motion rate ( $\dot{\omega}$ ) that resulted from the apsidal motion analysis were used for the preliminary light curve analysis.
3. Then the inclination ( $i$ ) from the LC analysis was used for the final apsidal motion analysis.
4. And finally, the resulted  $e$ ,  $\omega$ , and  $\dot{\omega}$  values from the apsidal motion analysis were used for the final LC analysis.

In general, the differences between the preliminary results and the final ones as resulted from steps 1 and 3,

<sup>1</sup> [http://phoebe-project.org/1.0/docs/phoebe\\_manual.pdf](http://phoebe-project.org/1.0/docs/phoebe_manual.pdf)

and 2 and 4 are usually rather small. Moreover, this approach was a bit complicated because the minima times were also derived using the light curve template. Hence, the LC solution from step 2 allows us to derive the better times of minima for the step 3. The whole process runs iteratively until the changes are negligible (usually after running these four steps twice).

All of the times of minima were analysed using the method presented by Giménez & García-Pelayo (1983). This is a least-squares iterative procedure, including terms in the eccentricity up to the fifth order. There were five independent variables ( $T_0, P_s, e, \dot{\omega}, \omega_0$ ) derived. The argument of periastron  $\omega$  is then given by the linear equation  $\omega = \omega_0 + \dot{\omega} E$ , where  $\dot{\omega}$  is the rate of periastron advance,  $E$  is the epoch, and the position of periastron for the zero epoch  $T_0$  is denoted as  $\omega_0$ . The relation between the sidereal and the anomalistic periods,  $P_s$  and  $P_a$ , is then given by

$$P_s = P_a (1 - \dot{\omega}/360^\circ)$$

and the period of the apsidal motion is  $U = 360^\circ P_a / \dot{\omega}$ .

For all of the minima the individual weights were derived from their respective uncertainties. All of these data are stored in the online-only appendix (for a sample see Table 1).

## 5. NOTES ON INDIVIDUAL SYSTEMS

The eclipsing systems included in our analysis were proceeded in a similar way, hence we cannot focus on every star in detail. For some information and cross-identification of the stars see Table 2. For abbreviating the star names we used the notation used for the OGLE III survey for a better brevity, hence e.g. OGLE-LMC-ECL-07902 was shortened as #07902, etc. Only the most important results are summarized below in a few subsections. The final light curve fits, and the  $O - C$  diagrams are presented in Figs. 1 and 2; the parameters are given in Tables 3 and 4.

### 5.1. OGLE LMC-ECL-07902

For the only one system we found several spectroscopic data in the ESO archive. The star OGLE LMC-ECL-07902 was observed with the UVES (UV-Visual Echelle Spectrograph) during the ESO period 68 and 70 programmes. The exposure times were from 3300 to 3600 seconds, while the typical S/N ratios were from 12 to 35. All of the data were reduced using the standard ESO pipelines, and the final radial velocities (hereafter RV) used for the analysis were derived via a manual cross-correlation technique (i.e. the direct and flipped profile of the spectral lines manually shifted on the computer

screen to achieve the best match) using the program SPEFO (Horn et al. 1996; Škoda 1996) on several absorption lines (usually HeI lines in the region from 370 to 420 nm). The derived radial velocities are given in Table 5, however their respective errors are quite large due to weakness of some of the lines.

We solved simultaneously the RVs with the LCs in our solution. The final RV curve fit is presented in Fig. 3, while the parameters are given in Table 6. From this combined solution there resulted that the eclipsing masses are of about 6.8 and 4.4  $M_\odot$ , which is in very good agreement with the assumed fixed primary temperature  $T_1 = 20000$  K. As one can see, the final fit provides us with a solution which is far from the original assumption that the mass ratio  $q = 1$ . However, for the other systems the spectroscopy is unavailable and for deriving the mass ratio we have to use a method described above in section 3. Moreover, there was also discovered that the system shows an emission behavior (in all of the Balmer lines), but which remained fixed at a position of about  $+223$  km·s $^{-1}$ . If such an emission comes from the system or some other object in the same direction remains unsolved.

### 5.2. OGLE-LMC-ECL-20112

Definitely the most interesting seems to be the object #20112. We fixed the primary temperature at a value of 21000 K in agreement with a rough spectral estimation of B2V according to Zaritsky et al. (2004). With this temperature we found a LC solution (see Fig. 1), which was then used as a template to derive the individual minima times for a subsequent period analysis.

Analysing the available times of minima observations we found that there is also an additional variation after subtraction of the apsidal motion term in the  $O - C$  diagram, hence we can speculate that the system is probably a triple one. For the analysis we used a so-called 'light-travel time effect', see e.g. Irwin (1959), or Mayer (1990), simultaneously with the apsidal motion. The final plots with the fits are given in Fig.2, where one can see the final complete fit (noted as #20112 - a), only the apsidal motion fit (b), and only the third-body fit (c). The parameters are given in Table 7. Its 22-yr orbit is just being covered with the individual observations yet, however some new observations would be of great benefit for the hypothesis to be confirmed with higher conclusiveness.

From the third-body parameters, we are also able to compute the mass function of the distant component, which resulted in  $f(m_3) = 0.267 \pm 0.028 M_\odot$ . From this value, one can calculate a predicted minimal mass of the third body (i.e. assuming coplanar orbits  $i_3 = 90^\circ$ , and the masses of the eclipsing components  $M_1 + M_2 = 14 M_\odot$ ), which resulted in  $m_{3,min} = 4.5 M_\odot$ . The amplitude of radial velocity variation due to the third body resulted in about 7.7 km·s $^{-1}$ . If we propose such a body in the system, one can ask whether it is detectable somehow in the already obtained data. The period is long for continuous monitoring of the radial velocity changes, but detecting the third light in the light curve solution would be promising. Assuming a normal main sequence star, its luminosity would be of about  $L_{3,min} \approx 10\%$  of the total system luminosity. During our light curve fitting we detected a third light of about 7% of the total light,

TABLE 1  
LIST OF THE MINIMA TIMINGS USED FOR THE ANALYSIS.

Star	JD Hel.- 2400000	Error [day]	Type	Filter	Source / Observatory
OGLE-LMC-ECL-07902	48750.43767	0.00180	Prim	B+R	MACHO
OGLE-LMC-ECL-07902	48751.26899	0.00262	Sec	B+R	MACHO
OGLE-LMC-ECL-07902	49650.24560	0.00063	Prim	B+R	MACHO
OGLE-LMC-ECL-07902	49651.07718	0.00133	Sec	B+R	MACHO
OGLE-LMC-ECL-07902	49999.80063	0.00101	Prim	B+R	MACHO
OGLE-LMC-ECL-07902	50000.63238	0.00467	Sec	B+R	MACHO
...					

(This table is available in its entirety in the appendix section at the end, or via the CDS-tables.)

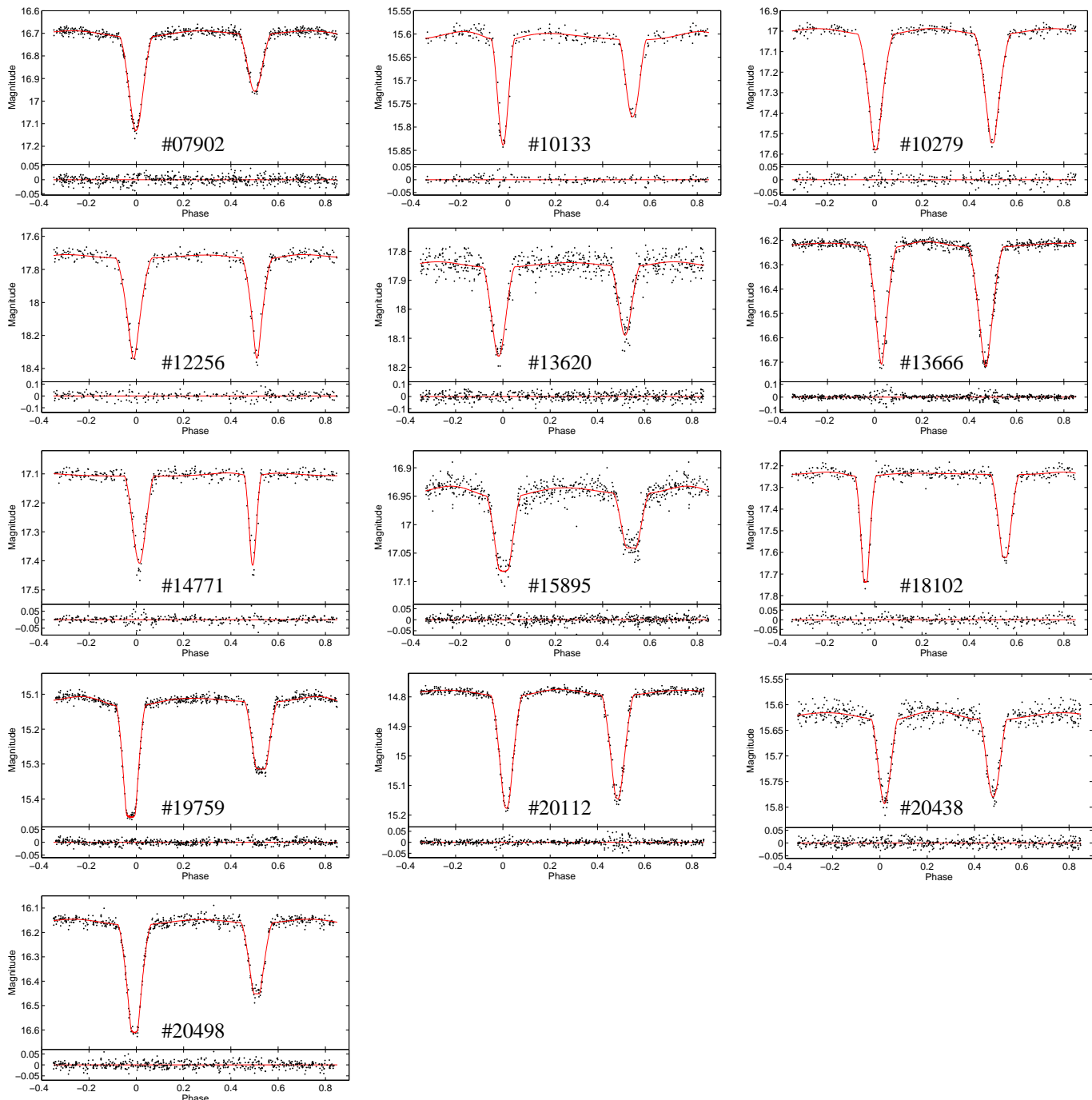


FIG. 1.— Light curves of the analysed systems, the data taken from the OGLE III survey, and the  $I$  filter. The bottom plots represent the residuals after subtraction of the fit.

however its uncertainty is quite large.

### 5.3. Systems with a third light

For several systems the detected value of the third light is rather high, so we can speculate about their triplicity. Of course, any such third light detection is not a direct evidence of a triple star, because the contributing component does not have to be necessarily bounded to the eclipsing system and can only be a so-called optical double. We detected a significant contribution of the third light (dominating above an error, i.e. a limit of about 5%) in 5 systems out of 13, i.e. in about 38% of the sample. However, even such a high number of the triple

candidates cannot easily be ruled out, because the fraction of triple systems for the stars of early spectral type is generally high, see e.g. Pribulla & Rucinski (2006), or Chini et al. (2012).

For #15895 the 56% contribution of the third light makes such a putative third component the dominant star in the system and the depths of both eclipses are due to this reason only very shallow. However, a variation in the  $O - C$  diagram is still rather difficult to detect here. The referee does not agree with the interpretation on system #15895. According to him the light curve of this system can be perfectly fitted without the third light for the mass ratio  $q \approx 0.3$ . However, we were not able to

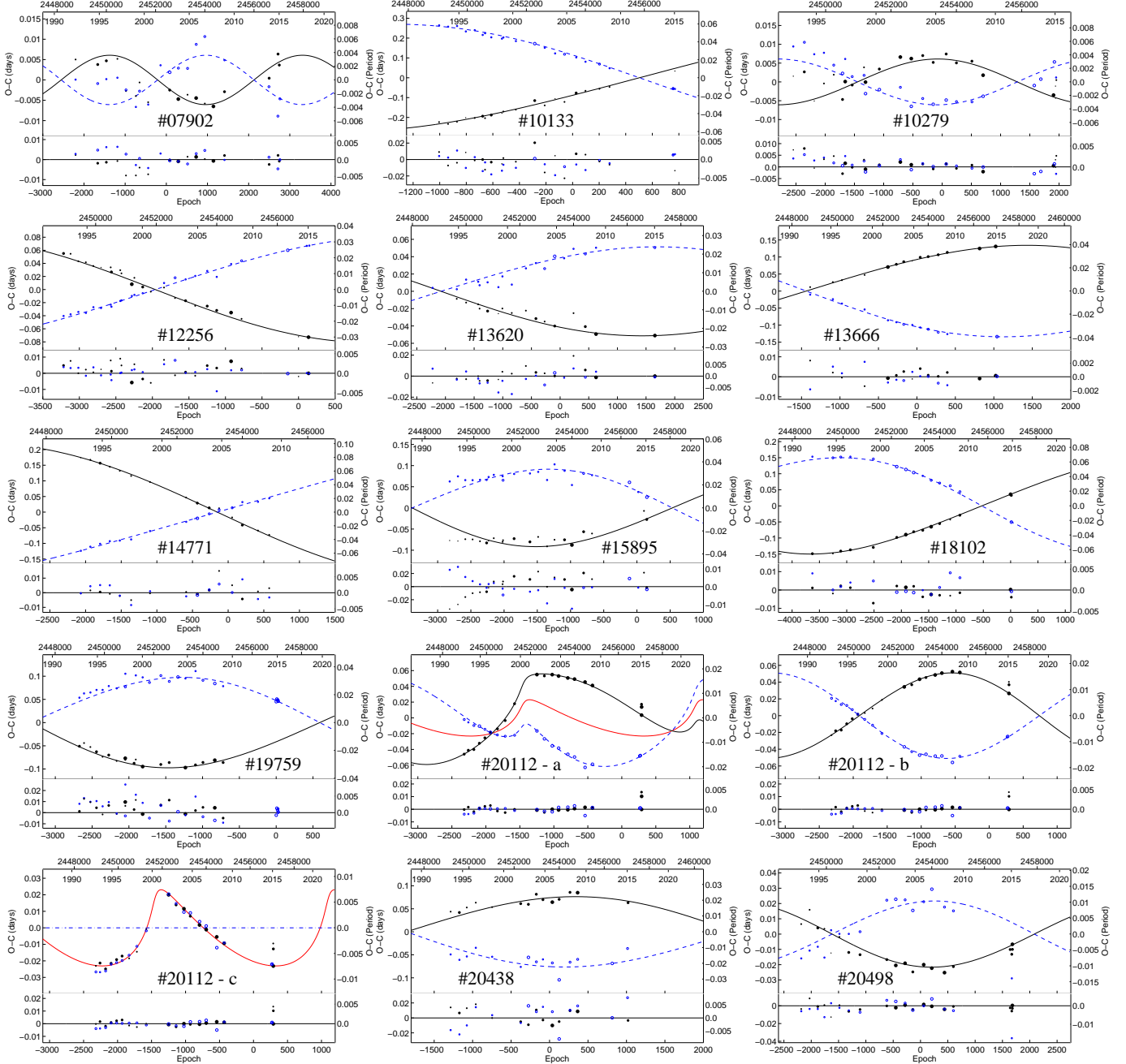


FIG. 2.—  $O - C$  diagrams for the times of minima of the analysed systems. The continuous and dashed curves represent predictions for the primary and secondary eclipses, respectively. The individual primary and secondary minima are denoted by dots and open circles, respectively. Larger symbols correspond to the more precise measurements. The bottom plots represent the residuals after subtraction of the fit.

reproduce such a result with the lowest rms.

#### 5.4. Other interesting systems

Some of the systems seem to show rather high scatter of residuals after subtracting the apsidal motion term. However, it cannot easily be described by a single periodic modulation or our data are too sparse and the time span is still rather short. Such systems are e.g. #07902, #10279, #13620, #14771, #20438, and #20498. The residuals plotted in Figure 2 show that the poor coverage of the data cannot allow us to derive any period or amplitude of such prospective modulation. Only more updated observations for these systems can help us to prove or reject any such hypothesis.

## 6. DISCUSSION AND CONCLUSIONS

We performed the first analysis of the apsidal motion and the LC fitting for thirteen early-type binary systems from the Large Magellanic Cloud. In our own Galaxy there are a few hundreds of apsidal motion eclipsing binaries known (Bulut & Demircan 2007); however, in other galaxies their number is still only very limited. Hence, this study still presents an important contribution to this topic. For some of the systems the presented apsidal motion hypothesis is still rather preliminary yet due to poor coverage of the  $O - C$  diagrams with the observations. For some others the fits as presented in Fig.2 are fairly reliable with the current data set.

TABLE 2  
IDENTIFICATION OF THE ANALYSED SYSTEMS.

System	OGLE II <sup>1</sup>	MACHO	RA	DE	$I_{\max}^2$	$(V - I)_0^3$	$(B - V)_0^4$
OGLE LMC-ECL-07902	SC13 257494	19.4423.464	05 <sup>h</sup> 07 <sup>m</sup> 24 <sup>s</sup> .60	-68°29′32″.4	16.69	-0.103	
OGLE LMC-ECL-10133	SC9 32388	79.5257.20	05 <sup>h</sup> 13 <sup>m</sup> 02 <sup>s</sup> .18	-69°19′39″.8	15.60	-0.167	-0.154
OGLE LMC-ECL-10279	SC9 115549	5.5376.2159	05 <sup>h</sup> 13 <sup>m</sup> 22 <sup>s</sup> .04	-69°27′24″.9	16.99	-0.278	-0.145
OGLE LMC-ECL-12256	SC7 120945	78.6096.420	05 <sup>h</sup> 18 <sup>m</sup> 15 <sup>s</sup> .55	-69°50′54″.2	17.71		-0.095
OGLE LMC-ECL-13620	SC6 323121	80.6708.5455	05 <sup>h</sup> 21 <sup>m</sup> 37 <sup>s</sup> .40	-69°24′20″.9	17.83	0.023	-0.187 <sup>5</sup>
OGLE LMC-ECL-13666	SC6 322419	78.6708.115	05 <sup>h</sup> 21 <sup>m</sup> 43 <sup>s</sup> .64	-69°24′42″.1	16.21	-0.214	-0.185
OGLE LMC-ECL-14771		3.7084.72	05 <sup>h</sup> 24 <sup>m</sup> 15 <sup>s</sup> .96	-68°31′20″.6	17.10	-0.209	-0.191
OGLE LMC-ECL-15895	SC4 296290	77.7548.414	05 <sup>h</sup> 26 <sup>m</sup> 49 <sup>s</sup> .26	-69°49′57″.2	16.93	0.120	-0.052
OGLE LMC-ECL-18102		82.8282.218	05 <sup>h</sup> 31 <sup>m</sup> 15 <sup>s</sup> .33	-69°20′25″.0	17.24	-0.167	-0.107
OGLE LMC-ECL-19759	SC16 70652	81.8881.44	05 <sup>h</sup> 35 <sup>m</sup> 02 <sup>s</sup> .02	-69°44′17″.9	15.11	-0.360	-0.245 <sup>5</sup>
OGLE LMC-ECL-20112		81.9003.27	05 <sup>h</sup> 35 <sup>m</sup> 49 <sup>s</sup> .13	-69°37′56″.6	14.78	-0.036	-0.226 <sup>5</sup>
OGLE LMC-ECL-20438		82.9130.43	05 <sup>h</sup> 36 <sup>m</sup> 27 <sup>s</sup> .18	-69°14′15″.4	15.61	-0.109	-0.257
OGLE LMC-ECL-20498		82.9131.80	05 <sup>h</sup> 36 <sup>m</sup> 35 <sup>s</sup> .07	-69°10′28″.2	16.15	-0.318	-0.265

Notes: [1] - The full name from the OGLE II survey should be OGLE LMC-SCn nnnnnn, [2] - Value taken from Graczyk et al. (2011), [3] - Value taken from Ulaczyk et al. (2012), [4] - Value derived from the (B-V) and (U-B) indices taken from Massey (2002), [5] Value taken from Zaritsky et al. (2004).

TABLE 3  
LIGHT CURVE PARAMETERS FOR THE ANALYSED SYSTEMS.

System	$T_1$ [K]	$T_2$ [K]	$i$ [deg]	$q = M_2/M_1$	$\Omega_1$	$\Omega_2$	$L_1$ [%]	$L_2$ [%]	$L_3$ [%]
#07902	20000 (fixed)	14166 (172)	83.28 (0.32)	0.65 (0.02)	4.466 (0.039)	4.885 (0.061)	77.4 (1.2)	20.7 (1.0)	1.9 (1.0)
#10133	16000 (fixed)	18463 (295)	77.75 (0.54)	1.05 (0.10)	5.989 (0.073)	7.152 (0.096)	53.2 (1.2)	44.8 (1.5)	2.0 (1.8)
#10279	15000 (fixed)	14587 (106)	87.57 (0.39)	0.86 (0.06)	4.661 (0.028)	5.154 (0.037)	62.2 (1.1)	37.8 (0.9)	0
#12256	12000 (fixed)	11768 (170)	87.67 (0.70)	1.08 (0.06)	6.183 (0.130)	5.669 (0.082)	43.4 (1.6)	56.6 (1.5)	0
#13620	18000 (fixed)	14462 (421)	83.22 (1.62)	0.68 (0.10)	4.795 (0.089)	5.337 (0.136)	61.7 (2.1)	20.5 (1.6)	17.8 (1.4)
#13666	18000 (fixed)	19124 (193)	84.39 (0.40)	1.08 (0.05)	5.868 (0.050)	5.951 (0.046)	45.2 (1.0)	52.8 (1.2)	2.0 (0.9)
#14771	18000 (fixed)	13601 (283)	83.87 (0.32)	0.61 (0.11)	6.358 (0.104)	6.186 (0.112)	72.1 (1.3)	25.9 (2.0)	2.0 (1.1)
#15895	10000 (fixed)	8406 (175)	89.79 (2.06)	0.60 (0.13)	4.042 (0.083)	4.925 (0.076)	35.7 (1.4)	7.9 (1.3)	56.4 (3.9)
#18102	12500 (fixed)	11245 (139)	88.18 (1.04)	0.73 (0.07)	6.052 (0.074)	6.705 (0.063)	70.7 (0.4)	29.3 (0.3)	0
#19759	20000 (fixed)	14424 (105)	87.99 (0.32)	0.50 (0.08)	4.334 (0.021)	4.792 (0.028)	82.6 (0.5)	15.3 (0.6)	2.1 (0.4)
#20112	21000 (fixed)	20199 (121)	84.06 (0.96)	0.78 (0.06)	4.803 (0.035)	5.649 (0.043)	64.9 (1.9)	28.2 (1.6)	6.8 (3.6)
#20438	25000 (fixed)	26172 (243)	75.85 (0.48)	1.00 (0.03)	5.629 (0.057)	6.206 (0.072)	49.0 (1.2)	41.2 (0.9)	9.8 (1.9)
#20498	25000 (fixed)	20373 (190)	89.77 (0.32)	0.63 (0.04)	4.602 (0.026)	4.848 (0.036)	69.3 (0.7)	22.5 (0.3)	8.2 (0.8)

TABLE 4  
THE PARAMETERS OF THE APSIDAL MOTION FOR THE INDIVIDUAL SYSTEMS.

System	$T_0 - 2400000$ [HJD]	$P_s$ [days]	$e$	$\dot{\omega}$ [deg/cycle]	$\omega_0$ [deg]	$U$ [yr]
#07902	52436.6397 (8)	1.6725077 (5)	0.011 (3)	0.0769 (110)	286.2 (1.5)	21.4 (3.6)
#10133	53566.7152 (31)	4.5023648 (52)	0.194 (58)	0.0413 (56)	68.2 (5.4)	107.4 (16.8)
#10279	53564.1812 (8)	1.7883577 (5)	0.011 (3)	0.0658 (83)	185.3 (2.4)	26.8 (3.8)
#12256	56701.5995 (115)	2.4137033 (53)	0.105 (24)	0.0283 (32)	326.2 (3.3)	84.2 (10.6)
#13620	53500.4749 (60)	2.1350145 (53)	0.075 (20)	0.0247 (70)	321.4 (5.1)	85.1 (33.5)
#13666	53503.1465 (188)	3.3881128 (27)	0.124 (36)	0.0332 (65)	137.7 (2.9)	100.7 (24.4)
#14771	53564.9091 (220)	2.1804949(188)	0.295(172)	0.0242 (60)	273.7 (1.8)	88.8 (47.2)
#15895	56652.5199 (239)	2.7098695(115)	0.106 (25)	0.0459 (99)	65.5 (7.7)	58.1 (16.2)
#18102	56945.0581 (425)	2.2650335(196)	0.206 (64)	0.0314 (47)	106.5 (3.4)	71.1 (12.4)
#19759	56974.3200 (252)	2.9895026 (14)	0.102 (24)	0.0459 (69)	62.8 (7.5)	64.2 (11.4)
#20112	56153.9786 (107)	3.0922295 (71)	0.051 (12)	0.0680 (35)	219.8 (5.5)	44.8 (2.2)
#20438	53572.6795 (131)	3.4134160 (28)	0.070 (20)	0.0422 (57)	168.6 (8.2)	79.6 (12.4)
#20498	53570.9957 (30)	2.0728518 (23)	0.033 (9)	0.0486 (80)	348.7 (2.7)	42.0 (8.3)

TABLE 5  
 LIST OF THE RADIAL VELOCITIES USED FOR THE ANALYSIS.

Star	JD Hel.- 2400000	$RV_1$ [km s <sup>-1</sup> ]	error $RV_1$ [km s <sup>-1</sup> ]	$RV_2$ [km s <sup>-1</sup> ]	error $RV_2$ [km s <sup>-1</sup> ]
OGLE-LMC-ECL-07902	52249.27501	125.54	5.66	532.14	18.14
OGLE-LMC-ECL-07902	52249.31372	133.95	6.30	513.63	15.03
OGLE-LMC-ECL-07902	52250.22672	412.18	2.81	93.63	11.58
OGLE-LMC-ECL-07902	52250.18798	428.65	4.09	68.18	11.26
OGLE-LMC-ECL-07902	52622.04155	159.93	7.20	493.02	12.92

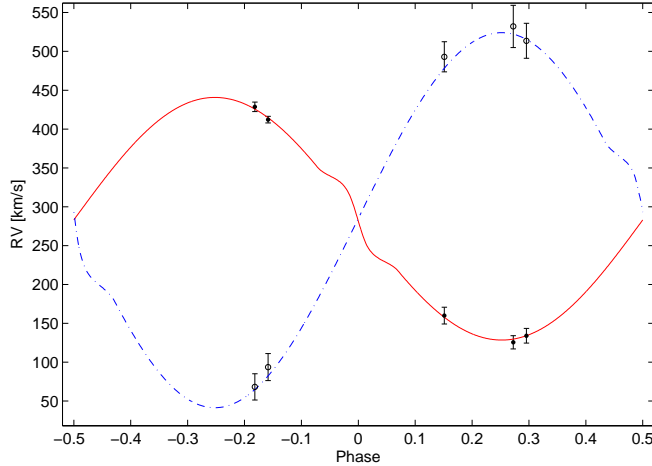


FIG. 3.— Radial velocity curves for the system OGLE LMC-ECL-07902 as derived from the ESO data, see the text for details.

For the system #20112 we presented a third-body hypothesis, which resulted from the analysis of residuals after subtracting the apsidal motion term in the  $O-C$  diagram. Its 22-yr variation is still preliminary, and should be confirmed via dedicated new observations in upcoming years. We also presented a few more similar systems, which are suspicious to be also triples, but for which

 TABLE 6  
 RADIAL VELOCITY FIT FOR #07902.

Parameter [Unit]	Value
$A$ [ $R_\odot$ ]	$13.26 \pm 0.05$
$q$ ( $=M_2/M_1$ )	$0.65 \pm 0.02$
$\gamma$ [km/s]	$283.9 \pm 0.4$
Derived quantities:	
$M_1$ [ $M_\odot$ ]	$6.8 \pm 0.5$
$M_2$ [ $M_\odot$ ]	$4.4 \pm 0.4$
$R_1$ [ $R_\odot$ ]	$3.5 \pm 0.2$
$R_2$ [ $R_\odot$ ]	$2.3 \pm 0.2$

 TABLE 7  
 THIRD-BODY ORBIT PARAMETERS FOR #20112.

Parameter [Unit]	Value
$p_3$ [yr]	$21.6 \pm 7.1$
$A_3$ [day]	$0.0230 \pm 0.0087$
$T_3$ [HJD]	$2459536 \pm 1121$
$e_3$	$0.743 \pm 0.088$
$\omega_3$ [deg]	$35.9 \pm 9.0$

much more observations are needed.

There also resulted that the presented apsidal and light curve analysis without any spectroscopic information cannot be used for testing the evolutionary stellar models via deriving the internal structure constant values. Their errors are too high and a more thorough analysis with some radial velocities would be needed. Some of the presented stars are bright enough for a spectral monitoring, hence we encourage the observers to obtain new, high-dispersion, and high-S/N spectroscopic observations. Using these data and methods like spectral disentangling can help us to construct the radial velocity curves of both components, confirm the apsidal motion hypothesis, test the stellar structure models, or detect the third bodies, as indicated from our analysis. The same apply for testing the models for slightly different chemical composition of LMC stars (e.g. Ribas 2004). Much better data are needed, however our presented analysis can serve as a starting point for these dedicated observations.

We do thank the MACHO and OGLE teams for making all of the observations easily public available. This work was supported by the Czech Science Foundation grants no. P209/10/0715, and GA15-02112S, and also by the student's project SVV-260089. We are also grateful to the ESO team at the La Silla Observatory for their help in maintaining and operating the Danish telescope. The following internet-based resources were used in research for this paper: the SIMBAD database and the VizieR service operated at the CDS, Strasbourg, France, and the NASA's Astrophysics Data System Bibliographic Services.

## REFERENCES

- Borkovits, T., Rappaport, S., Hajdu, T., & Sztakovics, J. 2015, MNRAS, 448, 946
- Bulut, I., & Demircan, O. 2007, MNRAS, 378, 179
- Chini, R., Hoffmeister, V. H., Nasserri, A., Stahl, O., & Zinnecker, H. 2012, MNRAS, 424, 1925
- Claret, A. 2005, A&A, 440, 647
- Davies, B., Kudritzki, R.-P., Gazak, Z., et al. 2015, ApJ, 806, 21
- Demarque, P., Woo, J.-H., Kim, Y.-C., & Yi, S. K. 2004, ApJS, 155, 667
- Faccioli, L., Alcock, C., Cook, K. et al. 2007, AJ, 134, 1963
- Giménez, A. 1994, ExA, 5, 91
- Giménez, A., & García-Pelayo, J.M. 1983, Ap&SS, 92, 203
- Graczyk, D. 2003, MNRAS, 342, 1334
- Graczyk, D., Soszyński, I., Poleski, R., et al. 2011, AcA, 61, 103
- Hong, K., Lee, C.-U., Kim, S.-L., & Kang, Y.-W. 2014, AJ, 147, 151
- Horn, J., Kubat, J., Harmanec, P., et al. 1996, A&A, 309, 521
- Irwin, J. B. 1959, AJ, 64, 149
- Johnson, H. L. 1958, Lowell Observatory Bulletin, 4, 37
- Kwee, K.K., & van Woerden, H. 1956, BAN, 12, 327
- Maeder, A. 1999, A&A, 347, 185
- Martins, F., & Palacios, A. 2013, A&A, 560, A16
- Massey, P. 2002, ApJS, 141, 81
- Mayer, P. 1990, BAICz, 41, 231
- Michalska, G. 2007, IBVS No. 5759
- Michalska, G. & Pigulski, A. 2005, A&A, 434, 89

- Pawlak, M., Graczyk, D., Soszyński, I., et al. 2013, *AcA*, 63, 323  
Paxton, B., Bildsten, L., Dotter, A., et al. 2011, *ApJS*, 192, 3  
Pecaut, M. J., & Mamajek, E. E. 2013, *ApJS*, 208, 9  
Pribulla, T., & Rucinski, S. M. 2006, *AJ*, 131, 2986  
Prša, A., & Zwitter, T. 2005, *ApJ*, 628, 426  
Ribas, I. 2004, *NewAR*, 48, 731  
Škoda, P. 1996, in *Astronomical Data Analysis Software and Systems V*, eds. G. H. Jacoby, & J. Barnes, ASP Conf. Ser., 101, 187  
Terrell, D., & Wilson, R. E. 2005, *Ap&SS*, 296, 221  
Ulaczyk, K., Szymański, M. K., Udalski, A., et al. 2012, *AcA*, 62, 247  
van Hamme, W. 1993, *AJ*, 106, 2096  
Westerlund, B. E. 1997, "The Magellanic Clouds", Cambridge University Press, UK  
Wilson, R. E., & Devinney, E. J. 1971, *ApJ*, 166, 605  
Wyrzykowski, L., Udalski, A., Kubiak, M., et al. 2004, *AcA*, 54, 1  
Zaritsky, D., Harris, J., Thompson, I. B., & Grebel, E. K. 2004, *AJ*, 128, 1606  
Zasche, P. & Wolf, M. 2013, *A&A*, 558, 51  
Zasche, P., Wolf, M., Vraštil, J., et al. 2014, *A&A*, 572, A71

APPENDIX  
TABLES OF MINIMA



TABLE 8  
LIST OF THE MINIMA TIMINGS USED FOR THE ANALYSIS.

Star	JD Hel.- 2400000	Error [day]	Type	Filter	Source / Observatory
OGLE-LMC-ECL-07902	48750.43767	0.00180	Prim	B+R	MACHO
OGLE-LMC-ECL-07902	48751.26899	0.00262	Sec	B+R	MACHO
OGLE-LMC-ECL-07902	49650.24560	0.00063	Prim	B+R	MACHO
OGLE-LMC-ECL-07902	49651.07718	0.00133	Sec	B+R	MACHO
OGLE-LMC-ECL-07902	49999.80063	0.00101	Prim	B+R	MACHO
OGLE-LMC-ECL-07902	50000.63238	0.00467	Sec	B+R	MACHO
OGLE-LMC-ECL-07902	50449.70569	0.00191	Prim	B+R	MACHO
OGLE-LMC-ECL-07902	50450.53731	0.00478	Sec	B+R	MACHO
OGLE-LMC-ECL-07902	51349.50906	0.00397	Prim	B+R	MACHO
OGLE-LMC-ECL-07902	51350.34318	0.00133	Sec	B+R	MACHO
OGLE-LMC-ECL-07902	50799.25190	0.00207	Prim	I	OGLE II
OGLE-LMC-ECL-07902	50800.08843	0.00129	Sec	I	OGLE II
OGLE-LMC-ECL-07902	51200.65253	0.00173	Prim	I	OGLE II
OGLE-LMC-ECL-07902	51201.48611	0.00244	Sec	I	OGLE II
OGLE-LMC-ECL-07902	51700.73081	0.00174	Prim	I	OGLE II
OGLE-LMC-ECL-07902	51701.56651	0.00321	Sec	I	OGLE II
OGLE-LMC-ECL-07902	52201.65596	0.00423	Sec	I	OGLE III
OGLE-LMC-ECL-07902	52575.45535	0.00071	Prim	I	OGLE III
OGLE-LMC-ECL-07902	52576.29597	0.00034	Sec	I	OGLE III
OGLE-LMC-ECL-07902	52925.00725	0.00046	Prim	I	OGLE III
OGLE-LMC-ECL-07902	52925.85112	0.00144	Sec	I	OGLE III
OGLE-LMC-ECL-07902	53299.65006	0.00155	Prim	I	OGLE III
OGLE-LMC-ECL-07902	53300.49278	0.00129	Sec	I	OGLE III
OGLE-LMC-ECL-07902	53649.20336	0.00032	Prim	I	OGLE III
OGLE-LMC-ECL-07902	53650.05280	0.00070	Sec	I	OGLE III
OGLE-LMC-ECL-07902	54000.42863	0.00201	Prim	I	OGLE III
OGLE-LMC-ECL-07902	54001.28134	0.00060	Sec	I	OGLE III
OGLE-LMC-ECL-07902	54349.98205	0.00030	Prim	I	OGLE III
OGLE-LMC-ECL-07902	54799.89023	0.00149	Prim	I	OGLE III
OGLE-LMC-ECL-07902	54800.73423	0.00157	Sec	I	OGLE III
OGLE-LMC-ECL-07902	56608.70858	0.00099	Sec	R	DK154
OGLE-LMC-ECL-07902	56614.56445	0.00079	Prim	R	DK154
OGLE-LMC-ECL-07902	56971.63552	0.00085	Sec	R	DK154
OGLE-LMC-ECL-07902	56975.83205	0.00119	Prim	R	DK154
OGLE-LMC-ECL-07902	57027.67709	0.00090	Prim	R	DK154
OGLE-LMC-ECL-07902	57053.59265	0.00129	Sec	R	DK154
OGLE-LMC-ECL-10133	52283.42750	0.00396	Prim	I	OGLE III
OGLE-LMC-ECL-10133	52285.96599	0.00054	Sec	I	OGLE III
OGLE-LMC-ECL-10133	52621.08091	0.00697	Prim	I	OGLE III
OGLE-LMC-ECL-10133	52623.62263	0.00425	Sec	I	OGLE III
OGLE-LMC-ECL-10133	52972.29867	0.01157	Prim	I	OGLE III
OGLE-LMC-ECL-10133	52974.77879	0.00428	Sec	I	OGLE III
OGLE-LMC-ECL-10133	53291.95111	0.00448	Prim	I	OGLE III
OGLE-LMC-ECL-10133	53294.44267	0.00352	Sec	I	OGLE III
OGLE-LMC-ECL-10133	53688.20416	0.00395	Prim	I	OGLE III
OGLE-LMC-ECL-10133	53690.63503	0.00659	Sec	I	OGLE III
OGLE-LMC-ECL-10133	54003.38087	0.00951	Prim	I	OGLE III
OGLE-LMC-ECL-10133	54005.77866	0.00463	Sec	I	OGLE III
OGLE-LMC-ECL-10133	54476.13926	0.00598	Prim	I	OGLE III
OGLE-LMC-ECL-10133	54478.51529	0.00173	Sec	I	OGLE III
OGLE-LMC-ECL-10133	54818.32862	0.00928	Prim	I	OGLE III
OGLE-LMC-ECL-10133	54820.67411	0.00462	Sec	I	OGLE III
OGLE-LMC-ECL-10133	50518.42151	0.00202	Prim	I	OGLE II
OGLE-LMC-ECL-10133	50521.08229	0.00589	Sec	I	OGLE II
OGLE-LMC-ECL-10133	50811.08100	0.00343	Prim	I	OGLE II
OGLE-LMC-ECL-10133	50813.72398	0.00796	Sec	I	OGLE II
OGLE-LMC-ECL-10133	51220.81424	0.00545	Prim	I	OGLE II
OGLE-LMC-ECL-10133	51223.43846	0.01620	Sec	I	OGLE II
OGLE-LMC-ECL-10133	51644.04625	0.00432	Prim	I	OGLE II
OGLE-LMC-ECL-10133	51646.64283	0.00906	Sec	I	OGLE II
OGLE-LMC-ECL-10133	49041.61566	0.00650	Prim	B+R	MACHO
OGLE-LMC-ECL-10133	49044.35420	0.01014	Sec	B+R	MACHO
OGLE-LMC-ECL-10133	49347.76725	0.00927	Prim	B+R	MACHO
OGLE-LMC-ECL-10133	49350.50869	0.00921	Sec	B+R	MACHO
OGLE-LMC-ECL-10133	49649.43670	0.00738	Prim	B+R	MACHO
OGLE-LMC-ECL-10133	49652.17045	0.01600	Sec	B+R	MACHO
OGLE-LMC-ECL-10133	49946.61326	0.01300	Prim	B+R	MACHO
OGLE-LMC-ECL-10133	49949.29942	0.00782	Sec	B+R	MACHO
OGLE-LMC-ECL-10133	50248.27053	0.00676	Prim	B+R	MACHO
OGLE-LMC-ECL-10133	50250.96420	0.00928	Sec	B+R	MACHO
OGLE-LMC-ECL-10133	50599.45414	0.00979	Prim	B+R	MACHO
OGLE-LMC-ECL-10133	50602.13333	0.02528	Sec	B+R	MACHO
OGLE-LMC-ECL-10133	51171.27955	0.01578	Prim	B+R	MACHO
OGLE-LMC-ECL-10133	51173.90678	0.00681	Sec	B+R	MACHO
OGLE-LMC-ECL-10133	56972.70306	0.00315	Sec	R	DK154
OGLE-LMC-ECL-10133	56972.70371	0.00197	Sec	R	DK154
OGLE-LMC-ECL-10133	57033.57280	0.00443	Prim	R	DK154
OGLE-LMC-ECL-10133	57035.73398	0.00312	Sec	R	DK154
OGLE-LMC-ECL-10279	52285.51202	0.00043	Prim	I	OGLE III
OGLE-LMC-ECL-10279	52286.39815	0.00126	Sec	I	OGLE III

TABLE 9  
LIST OF THE MINIMA TIMINGS USED FOR THE ANALYSIS - CONT.

Star	JD Hel.- 2400000	Error [day]	Type	Filter	Source / Observatory
OGLE-LMC-ECL-10279	52619.93450	0.00073	Prim	I	OGLE III
OGLE-LMC-ECL-10279	52620.81597	0.00056	Sec	I	OGLE III
OGLE-LMC-ECL-10279	52970.45341	0.00113	Prim	I	OGLE III
OGLE-LMC-ECL-10279	52971.33617	0.00168	Sec	I	OGLE III
OGLE-LMC-ECL-10279	53290.56763	0.00107	Prim	I	OGLE III
OGLE-LMC-ECL-10279	53291.45068	0.00091	Sec	I	OGLE III
OGLE-LMC-ECL-10279	53687.58529	0.00120	Prim	I	OGLE III
OGLE-LMC-ECL-10279	53688.46721	0.00048	Sec	I	OGLE III
OGLE-LMC-ECL-10279	54002.33388	0.00109	Prim	I	OGLE III
OGLE-LMC-ECL-10279	54003.21775	0.00204	Sec	I	OGLE III
OGLE-LMC-ECL-10279	54476.24913	0.00107	Prim	I	OGLE III
OGLE-LMC-ECL-10279	54477.13249	0.00173	Sec	I	OGLE III
OGLE-LMC-ECL-10279	54817.82173	0.00062	Prim	I	OGLE III
OGLE-LMC-ECL-10279	54818.71031	0.00050	Sec	I	OGLE III
OGLE-LMC-ECL-10279	50516.81496	0.00124	Prim	I	OGLE II
OGLE-LMC-ECL-10279	50517.71608	0.00078	Sec	I	OGLE II
OGLE-LMC-ECL-10279	50811.89782	0.00140	Prim	I	OGLE II
OGLE-LMC-ECL-10279	50812.79423	0.00179	Sec	I	OGLE II
OGLE-LMC-ECL-10279	51219.64415	0.00025	Prim	I	OGLE II
OGLE-LMC-ECL-10279	51220.53527	0.00054	Sec	I	OGLE II
OGLE-LMC-ECL-10279	51643.48841	0.00116	Prim	I	OGLE II
OGLE-LMC-ECL-10279	51644.37713	0.00075	Sec	I	OGLE II
OGLE-LMC-ECL-10279	49011.02394	0.00790	Prim	B+R	MACHO
OGLE-LMC-ECL-10279	49011.92602	0.00253	Sec	B+R	MACHO
OGLE-LMC-ECL-10279	49349.02470	0.00154	Prim	B+R	MACHO
OGLE-LMC-ECL-10279	49349.92675	0.00204	Sec	B+R	MACHO
OGLE-LMC-ECL-10279	49651.24942	0.00750	Prim	B+R	MACHO
OGLE-LMC-ECL-10279	49652.15602	0.00595	Sec	B+R	MACHO
OGLE-LMC-ECL-10279	49948.12145	0.00286	Prim	B+R	MACHO
OGLE-LMC-ECL-10279	49949.02378	0.00996	Sec	B+R	MACHO
OGLE-LMC-ECL-10279	50248.56788	0.00317	Prim	B+R	MACHO
OGLE-LMC-ECL-10279	50249.46461	0.00211	Sec	B+R	MACHO
OGLE-LMC-ECL-10279	50599.08417	0.00084	Prim	B+R	MACHO
OGLE-LMC-ECL-10279	50599.98436	0.01153	Sec	B+R	MACHO
OGLE-LMC-ECL-10279	51174.93913	0.00297	Prim	B+R	MACHO
OGLE-LMC-ECL-10279	51175.83120	0.00192	Sec	B+R	MACHO
OGLE-LMC-ECL-10279	56383.52618	0.00085	Sec	R	DK154
OGLE-LMC-ECL-10279	56583.82393	0.00000	Sec	R	DK154
OGLE-LMC-ECL-10279	56972.78749	0.00047	Prim	R	DK154
OGLE-LMC-ECL-10279	56998.72750	0.00055	Sec	R	DK154
OGLE-LMC-ECL-10279	57031.80569	0.02887	Prim	R	DK154
OGLE-LMC-ECL-10279	57033.59083	0.00842	Prim	R	DK154
OGLE-LMC-ECL-10279	57050.58574	0.00436	Sec	R	DK154
OGLE-LMC-ECL-10279	57056.84431	0.00590	Prim	R	DK154
OGLE-LMC-ECL-12256	52257.97404	0.00552	Prim	I	OGLE III
OGLE-LMC-ECL-12256	52259.18778	0.00319	Sec	I	OGLE III
OGLE-LMC-ECL-12256	52622.42726	0.00337	Prim	I	OGLE III
OGLE-LMC-ECL-12256	52623.66506	0.00159	Sec	I	OGLE III
OGLE-LMC-ECL-12256	52969.99645	0.00095	Prim	I	OGLE III
OGLE-LMC-ECL-12256	52971.23588	0.00278	Sec	I	OGLE III
OGLE-LMC-ECL-12256	53288.59761	0.00454	Prim	I	OGLE III
OGLE-LMC-ECL-12256	53289.85007	0.00460	Sec	I	OGLE III
OGLE-LMC-ECL-12256	53684.44457	0.00243	Prim	I	OGLE III
OGLE-LMC-ECL-12256	53685.70515	0.00356	Sec	I	OGLE III
OGLE-LMC-ECL-12256	53998.21947	0.00209	Prim	I	OGLE III
OGLE-LMC-ECL-12256	53999.47755	0.00543	Sec	I	OGLE III
OGLE-LMC-ECL-12256	54473.71585	0.00080	Prim	I	OGLE III
OGLE-LMC-ECL-12256	54474.99689	0.00355	Sec	I	OGLE III
OGLE-LMC-ECL-12256	54818.86588	0.00258	Prim	I	OGLE III
OGLE-LMC-ECL-12256	54820.16145	0.00189	Sec	I	OGLE III
OGLE-LMC-ECL-12256	50520.13102	0.00211	Prim	I	OGLE II
OGLE-LMC-ECL-12256	50521.28478	0.00308	Sec	I	OGLE II
OGLE-LMC-ECL-12256	50812.19189	0.00401	Prim	I	OGLE II
OGLE-LMC-ECL-12256	50813.35170	0.00335	Sec	I	OGLE II
OGLE-LMC-ECL-12256	51193.53566	0.00072	Prim	I	OGLE II
OGLE-LMC-ECL-12256	51194.72450	0.00284	Sec	I	OGLE II
OGLE-LMC-ECL-12256	51553.17333	0.00157	Prim	I	OGLE II
OGLE-LMC-ECL-12256	51554.37058	0.00293	Sec	I	OGLE II
OGLE-LMC-ECL-12256	51821.08724	0.00443	Prim	I	OGLE II
OGLE-LMC-ECL-12256	51554.37058	0.00293	Sec	I	OGLE II
OGLE-LMC-ECL-12256	48939.18328	0.00229	Prim	B+R	MACHO
OGLE-LMC-ECL-12256	48940.29459	0.00429	Sec	B+R	MACHO
OGLE-LMC-ECL-12256	49170.89838	0.00428	Prim	B+R	MACHO
OGLE-LMC-ECL-12256	49172.01264	0.00754	Sec	B+R	MACHO
OGLE-LMC-ECL-12256	49426.73954	0.00418	Prim	B+R	MACHO
OGLE-LMC-ECL-12256	49427.86887	0.00296	Sec	B+R	MACHO
OGLE-LMC-ECL-12256	49675.34946	0.00561	Prim	B+R	MACHO
OGLE-LMC-ECL-12256	49676.47890	0.00871	Sec	B+R	MACHO
OGLE-LMC-ECL-12256	49923.95533	0.00445	Prim	B+R	MACHO
OGLE-LMC-ECL-12256	49925.09917	0.00847	Sec	B+R	MACHO

TABLE 10  
LIST OF THE MINIMA TIMINGS USED FOR THE ANALYSIS - CONT.

Star	JD Hel.- 2400000	Error [day]	Type	Filter	Source / Observatory
OGLE-LMC-ECL-12256	50177.39195	0.00802	Prim	B+R	MACHO
OGLE-LMC-ECL-12256	50178.53678	0.00466	Sec	B+R	MACHO
OGLE-LMC-ECL-12256	50496.00101	0.00661	Prim	B+R	MACHO
OGLE-LMC-ECL-12256	50497.15088	0.00429	Sec	B+R	MACHO
OGLE-LMC-ECL-12256	50850.80633	0.00673	Prim	B+R	MACHO
OGLE-LMC-ECL-12256	50851.97181	0.00872	Sec	B+R	MACHO
OGLE-LMC-ECL-12256	51278.02511	0.00305	Prim	B+R	MACHO
OGLE-LMC-ECL-12256	51279.20583	0.00481	Sec	B+R	MACHO
OGLE-LMC-ECL-12256	56345.63853	0.00079	Sec	R	DK154
OGLE-LMC-ECL-12256	56701.52767	0.01220	Prim	R	DK154
OGLE-LMC-ECL-12256	56975.62188	0.01757	Sec	R	DK154
OGLE-LMC-ECL-12256	57029.79059	0.00015	Prim	R	DK154
OGLE-LMC-ECL-12256	57057.68825	0.00588	Sec	R	DK154
OGLE-LMC-ECL-13620	48750.06458	0.00716	Prim	B+R	MACHO
OGLE-LMC-ECL-13620	48751.13908	0.01388	Sec	B+R	MACHO
OGLE-LMC-ECL-13620	49651.03505	0.00520	Prim	B+R	MACHO
OGLE-LMC-ECL-13620	49652.11366	0.00387	Sec	B+R	MACHO
OGLE-LMC-ECL-13620	49999.03806	0.00474	Prim	B+R	MACHO
OGLE-LMC-ECL-13620	50000.13212	0.00983	Sec	B+R	MACHO
OGLE-LMC-ECL-13620	50449.52412	0.00647	Prim	B+R	MACHO
OGLE-LMC-ECL-13620	50450.61769	0.00695	Sec	B+R	MACHO
OGLE-LMC-ECL-13620	51350.49545	0.00653	Prim	B+R	MACHO
OGLE-LMC-ECL-13620	51351.60003	0.00846	Sec	B+R	MACHO
OGLE-LMC-ECL-13620	50500.75955	0.00613	Prim	I	OGLE II
OGLE-LMC-ECL-13620	50501.85405	0.00498	Sec	I	OGLE II
OGLE-LMC-ECL-13620	50799.65873	0.00203	Prim	I	OGLE II
OGLE-LMC-ECL-13620	50800.75949	0.00579	Sec	I	OGLE II
OGLE-LMC-ECL-13620	51201.03850	0.00895	Prim	I	OGLE II
OGLE-LMC-ECL-13620	51202.13661	0.01010	Sec	I	OGLE II
OGLE-LMC-ECL-13620	51700.63267	0.00630	Prim	I	OGLE II
OGLE-LMC-ECL-13620	51701.73293	0.01224	Sec	I	OGLE II
OGLE-LMC-ECL-13620	52225.84891	0.00395	Prim	I	OGLE III
OGLE-LMC-ECL-13620	52226.96530	0.00561	Sec	I	OGLE III
OGLE-LMC-ECL-13620	52599.46726	0.00174	Prim	I	OGLE III
OGLE-LMC-ECL-13620	52600.59886	0.00637	Sec	I	OGLE III
OGLE-LMC-ECL-13620	52923.98609	0.00258	Prim	I	OGLE III
OGLE-LMC-ECL-13620	52925.11474	0.00208	Sec	I	OGLE III
OGLE-LMC-ECL-13620	53299.74348	0.00096	Prim	I	OGLE III
OGLE-LMC-ECL-13620	53300.89148	0.00000	Sec	I	OGLE III
OGLE-LMC-ECL-13620	53299.74348	0.00096	Prim	I	OGLE III
OGLE-LMC-ECL-13620	53651.03161	0.00286	Sec	I	OGLE III
OGLE-LMC-ECL-13620	54000.04313	0.00530	Prim	I	OGLE III
OGLE-LMC-ECL-13620	54001.18487	0.00439	Sec	I	OGLE III
OGLE-LMC-ECL-13620	54439.84054	0.00235	Prim	I	OGLE III
OGLE-LMC-ECL-13620	54440.99195	0.00181	Sec	I	OGLE III
OGLE-LMC-ECL-13620	54839.07964	0.00064	Prim	I	OGLE III
OGLE-LMC-ECL-13620	54840.24687	0.00434	Sec	I	OGLE III
OGLE-LMC-ECL-13620	57028.63689	0.00100	Sec	R	DK154
OGLE-LMC-ECL-13620	57031.73783	0.00077	Prim	R	DK154
OGLE-LMC-ECL-13666	48800.45764	0.00368	Prim	B+R	MACHO
OGLE-LMC-ECL-13666	48802.12942	0.00774	Sec	B+R	MACHO
OGLE-LMC-ECL-13666	49799.96551	0.00587	Prim	B+R	MACHO
OGLE-LMC-ECL-13666	49801.60936	0.00445	Sec	B+R	MACHO
OGLE-LMC-ECL-13666	50199.76844	0.00428	Prim	B+R	MACHO
OGLE-LMC-ECL-13666	50201.39370	0.00526	Sec	B+R	MACHO
OGLE-LMC-ECL-13666	51199.27717	0.00314	Prim	B+R	MACHO
OGLE-LMC-ECL-13666	51200.86972	0.00441	Sec	B+R	MACHO
OGLE-LMC-ECL-13666	52225.89852	0.00053	Prim	I	OGLE III
OGLE-LMC-ECL-13666	52227.43622	0.00429	Sec	I	OGLE III
OGLE-LMC-ECL-13666	52598.59894	0.00198	Prim	I	OGLE III
OGLE-LMC-ECL-13666	52600.12301	0.00248	Sec	I	OGLE III
OGLE-LMC-ECL-13666	52923.86521	0.00127	Prim	I	OGLE III
OGLE-LMC-ECL-13666	52925.37570	0.00231	Sec	I	OGLE III
OGLE-LMC-ECL-13666	53299.94817	0.00921	Prim	I	OGLE III
OGLE-LMC-ECL-13666	53301.45429	0.00248	Sec	I	OGLE III
OGLE-LMC-ECL-13666	53648.93441	0.00176	Prim	I	OGLE III
OGLE-LMC-ECL-13666	53650.42244	0.00254	Sec	I	OGLE III
OGLE-LMC-ECL-13666	54001.30010	0.00202	Prim	I	OGLE III
OGLE-LMC-ECL-13666	54002.78112	0.00102	Sec	I	OGLE III
OGLE-LMC-ECL-13666	54441.76027	0.00204	Prim	I	OGLE III
OGLE-LMC-ECL-13666	54443.22696	0.00230	Sec	I	OGLE III
OGLE-LMC-ECL-13666	54841.56466	0.00163	Prim	I	OGLE III
OGLE-LMC-ECL-13666	54843.01890	0.00274	Sec	I	OGLE III
OGLE-LMC-ECL-13666	56264.58338	0.00038	Prim	R	DK154
OGLE-LMC-ECL-13666	56972.70509	0.00036	Prim	R	DK154
OGLE-LMC-ECL-13666	57031.73211	0.00053	Sec	R	DK154
OGLE-LMC-ECL-14771	52280.64360	0.00255	Prim	I	OGLE III
OGLE-LMC-ECL-14771	52281.65623	0.00277	Sec	I	OGLE III
OGLE-LMC-ECL-14771	52622.96379	0.00107	Prim	I	OGLE III
OGLE-LMC-ECL-14771	52624.00532	0.00084	Sec	I	OGLE III

TABLE 11  
LIST OF THE MINIMA TIMINGS USED FOR THE ANALYSIS - CONT.

Star	JD Hel.- 2400000	Error [day]	Type	Filter	Source / Observatory
OGLE-LMC-ECL-14771	52984.91102	0.00124	Prim	I	OGLE III
OGLE-LMC-ECL-14771	52985.98211	0.00222	Sec	I	OGLE III
OGLE-LMC-ECL-14771	53287.99846	0.00545	Prim	I	OGLE III
OGLE-LMC-ECL-14771	53289.08411	0.00166	Sec	I	OGLE III
OGLE-LMC-ECL-14771	53687.00004	0.00496	Prim	I	OGLE III
OGLE-LMC-ECL-14771	53688.12111	0.00131	Sec	I	OGLE III
OGLE-LMC-ECL-14771	53998.78656	0.00190	Prim	I	OGLE III
OGLE-LMC-ECL-14771	53999.95047	0.00505	Sec	I	OGLE III
OGLE-LMC-ECL-14771	54476.29771	0.00287	Prim	I	OGLE III
OGLE-LMC-ECL-14771	54477.47995	0.00272	Sec	I	OGLE III
OGLE-LMC-ECL-14771	54820.80242	0.00488	Prim	I	OGLE III
OGLE-LMC-ECL-14771	54822.00975	0.01181	Sec	I	OGLE III
OGLE-LMC-ECL-14771	49057.99767	0.00844	Prim	B+R	MACHO
OGLE-LMC-ECL-14771	49058.79013	0.00421	Sec	B+R	MACHO
OGLE-LMC-ECL-14771	49350.17760	0.00353	Prim	B+R	MACHO
OGLE-LMC-ECL-14771	49350.98966	0.00400	Sec	B+R	MACHO
OGLE-LMC-ECL-14771	49648.89471	0.00193	Prim	B+R	MACHO
OGLE-LMC-ECL-14771	49649.72701	0.00617	Sec	B+R	MACHO
OGLE-LMC-ECL-14771	49945.43060	0.00449	Prim	B+R	MACHO
OGLE-LMC-ECL-14771	49946.28295	0.00343	Sec	B+R	MACHO
OGLE-LMC-ECL-14771	50250.68726	0.00517	Prim	B+R	MACHO
OGLE-LMC-ECL-14771	50251.55429	0.00289	Sec	B+R	MACHO
OGLE-LMC-ECL-14771	50597.36981	0.00402	Prim	B+R	MACHO
OGLE-LMC-ECL-14771	50598.25695	0.00446	Sec	B+R	MACHO
OGLE-LMC-ECL-14771	51175.18171	0.00263	Prim	B+R	MACHO
OGLE-LMC-ECL-14771	51176.11505	0.00576	Sec	B+R	MACHO
OGLE-LMC-ECL-15895	52286.83982	0.00395	Prim	I	OGLE III
OGLE-LMC-ECL-15895	52288.35649	0.01024	Sec	I	OGLE III
OGLE-LMC-ECL-15895	52622.87535	0.00658	Prim	I	OGLE III
OGLE-LMC-ECL-15895	52624.38414	0.00427	Sec	I	OGLE III
OGLE-LMC-ECL-15895	52985.97548	0.00674	Prim	I	OGLE III
OGLE-LMC-ECL-15895	52987.48739	0.00599	Sec	I	OGLE III
OGLE-LMC-ECL-15895	53289.49664	0.00734	Prim	I	OGLE III
OGLE-LMC-ECL-15895	53291.02978	0.00679	Sec	I	OGLE III
OGLE-LMC-ECL-15895	53698.68683	0.00312	Prim	I	OGLE III
OGLE-LMC-ECL-15895	53700.20491	0.01472	Sec	I	OGLE III
OGLE-LMC-ECL-15895	53999.46999	0.00098	Prim	I	OGLE III
OGLE-LMC-ECL-15895	54000.96672	0.02676	Sec	I	OGLE III
OGLE-LMC-ECL-15895	54476.43833	0.00346	Prim	I	OGLE III
OGLE-LMC-ECL-15895	54477.93117	0.00358	Sec	I	OGLE III
OGLE-LMC-ECL-15895	54820.58754	0.00527	Prim	I	OGLE III
OGLE-LMC-ECL-15895	54822.08051	0.01040	Sec	I	OGLE III
OGLE-LMC-ECL-15895	50520.00247	0.00258	Prim	I	OGLE II
OGLE-LMC-ECL-15895	50521.50625	0.00583	Sec	I	OGLE II
OGLE-LMC-ECL-15895	50812.67954	0.00443	Prim	I	OGLE II
OGLE-LMC-ECL-15895	50814.18421	0.01134	Sec	I	OGLE II
OGLE-LMC-ECL-15895	51189.34664	0.00738	Prim	I	OGLE II
OGLE-LMC-ECL-15895	51190.84344	0.00350	Sec	I	OGLE II
OGLE-LMC-ECL-15895	51641.89855	0.00324	Prim	I	OGLE II
OGLE-LMC-ECL-15895	51643.40644	0.00566	Sec	I	OGLE II
OGLE-LMC-ECL-15895	49013.32079	0.01350	Prim	B+R	MACHO
OGLE-LMC-ECL-15895	49014.81532	0.00909	Sec	B+R	MACHO
OGLE-LMC-ECL-15895	49349.34333	0.01711	Prim	B+R	MACHO
OGLE-LMC-ECL-15895	49350.85120	0.01012	Sec	B+R	MACHO
OGLE-LMC-ECL-15895	49650.14314	0.00794	Prim	B+R	MACHO
OGLE-LMC-ECL-15895	49651.63787	0.02090	Sec	B+R	MACHO
OGLE-LMC-ECL-15895	49948.22828	0.01090	Prim	B+R	MACHO
OGLE-LMC-ECL-15895	49949.72329	0.01092	Sec	B+R	MACHO
OGLE-LMC-ECL-15895	50249.01942	0.00658	Prim	B+R	MACHO
OGLE-LMC-ECL-15895	50250.51965	0.00989	Sec	B+R	MACHO
OGLE-LMC-ECL-15895	50601.30330	0.01736	Prim	B+R	MACHO
OGLE-LMC-ECL-15895	50602.80940	0.01151	Sec	B+R	MACHO
OGLE-LMC-ECL-15895	51173.08349	0.00920	Prim	B+R	MACHO
OGLE-LMC-ECL-15895	51174.59363	0.02641	Sec	B+R	MACHO
OGLE-LMC-ECL-15895	56347.72008	0.00123	Sec	R	DK154
OGLE-LMC-ECL-15895	56705.39995	0.00449	Sec	R	DK154
OGLE-LMC-ECL-15895	56939.75894	0.00638	Prim	R	DK154
OGLE-LMC-ECL-15895	57053.55327	0.00195	Prim	R	DK154
OGLE-LMC-ECL-15895	57057.67081	0.00079	Sec	R	DK154
OGLE-LMC-ECL-18102	48725.10261	0.00390	Prim	B+R	MACHO
OGLE-LMC-ECL-18102	48726.53712	0.01530	Sec	B+R	MACHO
OGLE-LMC-ECL-18102	49574.49099	0.00429	Prim	B+R	MACHO
OGLE-LMC-ECL-18102	49575.92120	0.00278	Sec	B+R	MACHO
OGLE-LMC-ECL-18102	49900.66311	0.00189	Prim	B+R	MACHO
OGLE-LMC-ECL-18102	49902.08830	0.00155	Sec	B+R	MACHO
OGLE-LMC-ECL-18102	50299.31289	0.00219	Prim	B+R	MACHO
OGLE-LMC-ECL-18102	50300.73554	0.00620	Sec	B+R	MACHO
OGLE-LMC-ECL-18102	51250.63467	0.00279	Prim	B+R	MACHO
OGLE-LMC-ECL-18102	51252.04220	0.00398	Sec	B+R	MACHO
OGLE-LMC-ECL-18102	52224.63003	0.00000	Prim	I	OGLE III

TABLE 12  
LIST OF THE MINIMA TIMINGS USED FOR THE ANALYSIS - CONT.

Star	JD Hel.- 2400000	Error [day]	Type	Filter	Source / Observatory
OGLE-LMC-ECL-18102	52225.98281	0.00112	Sec	I	OGLE III
OGLE-LMC-ECL-18102	52600.63429	0.00138	Prim	I	OGLE III
OGLE-LMC-ECL-18102	52601.96959	0.00100	Sec	I	OGLE III
OGLE-LMC-ECL-18102	52924.54314	0.00155	Prim	I	OGLE III
OGLE-LMC-ECL-18102	52925.85973	0.00128	Sec	I	OGLE III
OGLE-LMC-ECL-18102	53300.54319	0.00194	Prim	I	OGLE III
OGLE-LMC-ECL-18102	53301.84519	0.00500	Sec	I	OGLE III
OGLE-LMC-ECL-18102	53649.36942	0.00131	Prim	I	OGLE III
OGLE-LMC-ECL-18102	53650.64646	0.00238	Sec	I	OGLE III
OGLE-LMC-ECL-18102	54000.45929	0.00204	Prim	I	OGLE III
OGLE-LMC-ECL-18102	54001.71805	0.00186	Sec	I	OGLE III
OGLE-LMC-ECL-18102	54439.88847	0.00481	Prim	I	OGLE III
OGLE-LMC-ECL-18102	54441.12600	0.00324	Sec	I	OGLE III
OGLE-LMC-ECL-18102	54840.81291	0.00313	Prim	I	OGLE III
OGLE-LMC-ECL-18102	54842.01847	0.00301	Sec	I	OGLE III
OGLE-LMC-ECL-18102	56942.82917	0.00035	Prim	R	DK154
OGLE-LMC-ECL-18102	56974.53643	0.00291	Prim	R	DK154
OGLE-LMC-ECL-18102	56975.58552	0.00150	Sec	R	DK154
OGLE-LMC-ECL-19759	48983.32857	0.00344	Prim	B+R	MACHO
OGLE-LMC-ECL-19759	48984.92795	0.01066	Sec	B+R	MACHO
OGLE-LMC-ECL-19759	49171.67416	0.00677	Prim	B+R	MACHO
OGLE-LMC-ECL-19759	49173.27577	0.01916	Sec	B+R	MACHO
OGLE-LMC-ECL-19759	49428.76274	0.00465	Prim	B+R	MACHO
OGLE-LMC-ECL-19759	49430.37499	0.03134	Sec	B+R	MACHO
OGLE-LMC-ECL-19759	49676.88127	0.00274	Prim	B+R	MACHO
OGLE-LMC-ECL-19759	49678.50924	0.00738	Sec	B+R	MACHO
OGLE-LMC-ECL-19759	49924.99918	0.00623	Prim	B+R	MACHO
OGLE-LMC-ECL-19759	49926.63793	0.00859	Sec	B+R	MACHO
OGLE-LMC-ECL-19759	50176.12105	0.00286	Prim	B+R	MACHO
OGLE-LMC-ECL-19759	50177.76446	0.00552	Sec	B+R	MACHO
OGLE-LMC-ECL-19759	50495.98508	0.00632	Prim	B+R	MACHO
OGLE-LMC-ECL-19759	50497.63632	0.00584	Sec	B+R	MACHO
OGLE-LMC-ECL-19759	50848.74883	0.00451	Prim	B+R	MACHO
OGLE-LMC-ECL-19759	50850.42920	0.01383	Sec	B+R	MACHO
OGLE-LMC-ECL-19759	51273.25886	0.01056	Prim	B+R	MACHO
OGLE-LMC-ECL-19759	51274.93496	0.00907	Sec	B+R	MACHO
OGLE-LMC-ECL-19759	50845.76286	0.00109	Prim	I	OGLE II
OGLE-LMC-ECL-19759	50847.41129	0.00250	Sec	I	OGLE II
OGLE-LMC-ECL-19759	51204.49224	0.00202	Prim	I	OGLE II
OGLE-LMC-ECL-19759	50847.41129	0.00250	Sec	I	OGLE II
OGLE-LMC-ECL-19759	51551.26748	0.00036	Prim	I	OGLE II
OGLE-LMC-ECL-19759	51552.95453	0.00475	Sec	I	OGLE II
OGLE-LMC-ECL-19759	51551.26748	0.00036	Prim	I	OGLE II
OGLE-LMC-ECL-19759	51827.97770	0.00321	Sec	I	OGLE II
OGLE-LMC-ECL-19759	52289.67922	0.00211	Prim	I	OGLE III
OGLE-LMC-ECL-19759	52291.36545	0.00179	Sec	I	OGLE III
OGLE-LMC-ECL-19759	52630.48662	0.00161	Prim	I	OGLE III
OGLE-LMC-ECL-19759	52632.15632	0.00179	Sec	I	OGLE III
OGLE-LMC-ECL-19759	52630.48662	0.00161	Prim	I	OGLE III
OGLE-LMC-ECL-19759	52987.91647	0.00049	Sec	I	OGLE III
OGLE-LMC-ECL-19759	53288.16629	0.00049	Prim	I	OGLE III
OGLE-LMC-ECL-19759	53289.85318	0.00520	Sec	I	OGLE III
OGLE-LMC-ECL-19759	53697.73384	0.00234	Prim	I	OGLE III
OGLE-LMC-ECL-19759	53699.43085	0.00597	Sec	I	OGLE III
OGLE-LMC-ECL-19759	53999.67901	0.00368	Prim	I	OGLE III
OGLE-LMC-ECL-19759	54001.35087	0.00251	Sec	I	OGLE III
OGLE-LMC-ECL-19759	54480.99372	0.00120	Prim	I	OGLE III
OGLE-LMC-ECL-19759	54482.65377	0.00117	Sec	I	OGLE III
OGLE-LMC-ECL-19759	54818.80260	0.00238	Prim	I	OGLE III
OGLE-LMC-ECL-19759	54820.46188	0.00774	Sec	I	OGLE III
OGLE-LMC-ECL-19759	56975.85980	0.00057	Sec	R	DK154
OGLE-LMC-ECL-19759	56999.78156	0.00134	Sec	R	DK154
OGLE-LMC-ECL-19759	57029.67427	0.00071	Sec	R	DK154
OGLE-LMC-ECL-19759	57050.60130	0.00174	Sec	R	DK154
OGLE-LMC-ECL-19759	57053.58734	0.00165	Sec	R	DK154
OGLE-LMC-ECL-19759	57056.57743	0.00077	Sec	R	DK154
OGLE-LMC-ECL-20112	48983.05231	0.00453	Prim	B+R	MACHO
OGLE-LMC-ECL-20112	48984.64237	0.00392	Sec	B+R	MACHO
OGLE-LMC-ECL-20112	49171.68324	0.00317	Prim	B+R	MACHO
OGLE-LMC-ECL-20112	49173.26482	0.01156	Sec	B+R	MACHO
OGLE-LMC-ECL-20112	49425.24699	0.00303	Prim	B+R	MACHO
OGLE-LMC-ECL-20112	49426.82362	0.00284	Sec	B+R	MACHO
OGLE-LMC-ECL-20112	49675.72555	0.00278	Prim	B+R	MACHO
OGLE-LMC-ECL-20112	49677.29340	0.00233	Sec	B+R	MACHO
OGLE-LMC-ECL-20112	49926.20303	0.00295	Prim	B+R	MACHO
OGLE-LMC-ECL-20112	49927.75999	0.00305	Sec	B+R	MACHO
OGLE-LMC-ECL-20112	50176.68045	0.00317	Prim	B+R	MACHO
OGLE-LMC-ECL-20112	50178.22672	0.00158	Sec	B+R	MACHO
OGLE-LMC-ECL-20112	50495.18467	0.00473	Prim	B+R	MACHO
OGLE-LMC-ECL-20112	50496.72310	0.00328	Sec	B+R	MACHO

TABLE 13  
LIST OF THE MINIMA TIMINGS USED FOR THE ANALYSIS - CONT.

Star	JD Hel.- 2400000	Error [day]	Type	Filter	Source / Observatory
OGLE-LMC-ECL-20112	50847.70940	0.00502	Prim	B+R	MACHO
OGLE-LMC-ECL-20112	50849.23561	0.00285	Sec	B+R	MACHO
OGLE-LMC-ECL-20112	51274.45833	0.00477	Prim	B+R	MACHO
OGLE-LMC-ECL-20112	51275.96449	0.00397	Sec	B+R	MACHO
OGLE-LMC-ECL-20112	52291.83887	0.00136	Prim	I	OGLE III
OGLE-LMC-ECL-20112	52293.31348	0.00089	Sec	I	OGLE III
OGLE-LMC-ECL-20112	52631.98245	0.00285	Prim	I	OGLE III
OGLE-LMC-ECL-20112	52633.44871	0.00174	Sec	I	OGLE III
OGLE-LMC-ECL-20112	52987.59048	0.00142	Prim	I	OGLE III
OGLE-LMC-ECL-20112	52989.04614	0.00083	Sec	I	OGLE III
OGLE-LMC-ECL-20112	53278.25823	0.00198	Prim	I	OGLE III
OGLE-LMC-ECL-20112	53279.71282	0.00051	Sec	I	OGLE III
OGLE-LMC-ECL-20112	53698.79902	0.00081	Prim	I	OGLE III
OGLE-LMC-ECL-20112	53700.24835	0.00097	Sec	I	OGLE III
OGLE-LMC-ECL-20112	54001.83603	0.00136	Prim	I	OGLE III
OGLE-LMC-ECL-20112	54003.28330	0.00116	Sec	I	OGLE III
OGLE-LMC-ECL-20112	54481.12794	0.00143	Prim	I	OGLE III
OGLE-LMC-ECL-20112	54482.56576	0.00084	Sec	I	OGLE III
OGLE-LMC-ECL-20112	54818.17657	0.00135	Prim	I	OGLE III
OGLE-LMC-ECL-20112	54819.62277	0.00158	Sec	I	OGLE III
OGLE-LMC-ECL-20112	56971.82498	0.00186	Sec	R	DK154
OGLE-LMC-ECL-20112	56999.65565	0.00120	Sec	R	DK154
OGLE-LMC-ECL-20112	57050.74241	0.00610	Prim	R	DK154
OGLE-LMC-ECL-20112	57053.82091	0.00016	Prim	R	DK154
OGLE-LMC-ECL-20112	57056.92344	0.00158	Prim	R	DK154
OGLE-LMC-ECL-20438	52292.70968	0.00485	Prim	I	OGLE III
OGLE-LMC-ECL-20438	52294.27894	0.01191	Sec	I	OGLE III
OGLE-LMC-ECL-20438	52634.04974	0.00320	Prim	I	OGLE III
OGLE-LMC-ECL-20438	52635.64122	0.00240	Sec	I	OGLE III
OGLE-LMC-ECL-20438	52985.65362	0.00407	Prim	I	OGLE III
OGLE-LMC-ECL-20438	52987.21342	0.00607	Sec	I	OGLE III
OGLE-LMC-ECL-20438	53279.19563	0.00404	Prim	I	OGLE III
OGLE-LMC-ECL-20438	53280.77250	0.00884	Sec	I	OGLE III
OGLE-LMC-ECL-20438	53695.62695	0.00235	Prim	I	OGLE III
OGLE-LMC-ECL-20438	53697.20161	0.00432	Sec	I	OGLE III
OGLE-LMC-ECL-20438	53999.42707	0.00329	Prim	I	OGLE III
OGLE-LMC-ECL-20438	54000.95887	0.00231	Sec	I	OGLE III
OGLE-LMC-ECL-20438	54480.73398	0.00331	Prim	I	OGLE III
OGLE-LMC-ECL-20438	54482.28889	0.00476	Sec	I	OGLE III
OGLE-LMC-ECL-20438	54818.66145	0.00217	Prim	I	OGLE III
OGLE-LMC-ECL-20438	54820.22326	0.00472	Sec	I	OGLE III
OGLE-LMC-ECL-20438	49183.07030	0.01084	Prim	B+R	MACHO
OGLE-LMC-ECL-20438	49184.68404	0.00815	Sec	B+R	MACHO
OGLE-LMC-ECL-20438	49572.19783	0.00422	Prim	B+R	MACHO
OGLE-LMC-ECL-20438	49573.80179	0.01102	Sec	B+R	MACHO
OGLE-LMC-ECL-20438	49899.89672	0.01767	Prim	B+R	MACHO
OGLE-LMC-ECL-20438	49901.49699	0.00923	Sec	B+R	MACHO
OGLE-LMC-ECL-20438	50299.27687	0.01249	Prim	B+R	MACHO
OGLE-LMC-ECL-20438	50300.88550	0.00990	Sec	B+R	MACHO
OGLE-LMC-ECL-20438	51026.32485	0.00779	Prim	B+R	MACHO
OGLE-LMC-ECL-20438	51027.92363	0.00699	Sec	B+R	MACHO
OGLE-LMC-ECL-20438	56352.83824	0.00112	Sec	R	DK154
OGLE-LMC-ECL-20438	57035.55385	0.00621	Sec	R	DK154
OGLE-LMC-ECL-20438	57057.84055	0.00282	Prim	R	DK154
OGLE-LMC-ECL-20498	52292.02945	0.00194	Prim	I	OGLE III
OGLE-LMC-ECL-20498	52293.10471	0.00282	Sec	I	OGLE III
OGLE-LMC-ECL-20498	52634.04620	0.00104	Prim	I	OGLE III
OGLE-LMC-ECL-20498	52635.12586	0.00109	Sec	I	OGLE III
OGLE-LMC-ECL-20498	52986.43240	0.00067	Prim	I	OGLE III
OGLE-LMC-ECL-20498	52987.51029	0.00239	Sec	I	OGLE III
OGLE-LMC-ECL-20498	53278.69882	0.00240	Prim	I	OGLE III
OGLE-LMC-ECL-20498	53279.77549	0.00098	Sec	I	OGLE III
OGLE-LMC-ECL-20498	53693.27394	0.00034	Prim	I	OGLE III
OGLE-LMC-ECL-20498	53694.35155	0.00170	Sec	I	OGLE III
OGLE-LMC-ECL-20498	54000.05373	0.00044	Prim	I	OGLE III
OGLE-LMC-ECL-20498	54001.14180	0.00141	Sec	I	OGLE III
OGLE-LMC-ECL-20498	54480.95241	0.00075	Prim	I	OGLE III
OGLE-LMC-ECL-20498	54482.03172	0.00166	Sec	I	OGLE III
OGLE-LMC-ECL-20498	54818.83122	0.00227	Prim	I	OGLE III
OGLE-LMC-ECL-20498	54819.90409	0.00268	Sec	I	OGLE III
OGLE-LMC-ECL-20498	48983.78048	0.00446	Prim	B+R	MACHO
OGLE-LMC-ECL-20498	48984.79031	0.00810	Sec	B+R	MACHO
OGLE-LMC-ECL-20498	49170.33789	0.00215	Prim	B+R	MACHO
OGLE-LMC-ECL-20498	49171.36065	0.00315	Sec	B+R	MACHO
OGLE-LMC-ECL-20498	49427.38354	0.00802	Prim	B+R	MACHO
OGLE-LMC-ECL-20498	49428.38902	0.00686	Sec	B+R	MACHO
OGLE-LMC-ECL-20498	49045.96676	0.00443	Prim	B+R	MACHO
OGLE-LMC-ECL-20498	49046.98074	0.00923	Sec	B+R	MACHO
OGLE-LMC-ECL-20498	49363.12242	0.01029	Prim	B+R	MACHO
OGLE-LMC-ECL-20498	49364.13217	0.00674	Sec	B+R	MACHO

TABLE 14  
LIST OF THE MINIMA TIMINGS USED FOR THE ANALYSIS - CONT.

Star	JD Hel.- 2400000	Error [day]	Type	Filter	Source / Observatory
OGLE-LMC-ECL-20498	49674.03832	0.00403	Prim	B+R	MACHO
OGLE-LMC-ECL-20498	49675.06246	0.00707	Sec	B+R	MACHO
OGLE-LMC-ECL-20498	49924.85282	0.00437	Prim	B+R	MACHO
OGLE-LMC-ECL-20498	49925.87046	0.00409	Sec	B+R	MACHO
OGLE-LMC-ECL-20498	50177.72492	0.01448	Prim	B+R	MACHO
OGLE-LMC-ECL-20498	50178.77624	0.00507	Sec	B+R	MACHO
OGLE-LMC-ECL-20498	50494.88176	0.00465	Prim	B+R	MACHO
OGLE-LMC-ECL-20498	50495.92021	0.00758	Sec	B+R	MACHO
OGLE-LMC-ECL-20498	50849.32928	0.00309	Prim	B+R	MACHO
OGLE-LMC-ECL-20498	50850.37785	0.00712	Sec	B+R	MACHO
OGLE-LMC-ECL-20498	51276.33528	0.00283	Prim	B+R	MACHO
OGLE-LMC-ECL-20498	51277.38675	0.00321	Sec	B+R	MACHO
OGLE-LMC-ECL-20498	56974.60825	0.00245	Prim	R	DK154
OGLE-LMC-ECL-20498	57034.71784	0.00306	Prim	R	DK154
OGLE-LMC-ECL-20498	57035.73851	0.01039	Sec	R	DK154
OGLE-LMC-ECL-20498	57057.52572	0.00039	Prim	R	DK154
OGLE-LMC-ECL-20498	57059.59527	0.00175	Prim	R	DK154